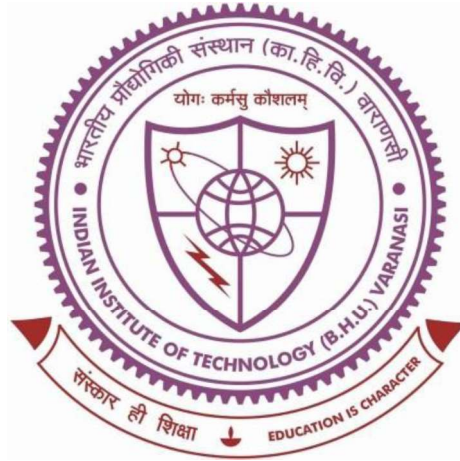


STUDIES ON EROSION WEAR CHARACTERISTICS OF DUAL PHASE STEEL



Thesis submitted in partial fulfillment for the
Award of Degree

Doctor of Philosophy

By

POOJA VERMA

DEPARTMENT OF MECHANICAL ENGINEERING
INDIAN INSTITUTE OF TECHNOLOGY
(BANARAS HINDU UNIVERSITY)
VARANASI - 221005

Roll No. 17131008

2023

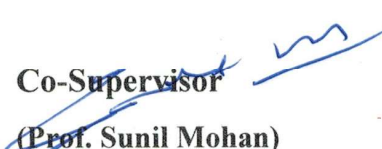
CERTIFICATE

This is to certify that the work contained in the thesis titled "*STUDIES ON EROSION WEAR CHARACTERISTICS OF DUAL PHASE STEEL*" by "*POOJA VERMA*" has been carried out under my/our supervision and that this work has not been submitted elsewhere for a degree.

It is further certified that the student has fulfilled all the requirements of Comprehensive Examination, Candidacy and SOTA for the award of Ph.D. Degree.



Supervisor
(Prof. Rajnesh Tyagi)
IIT (BHU), Varanasi
INDIA



Co-Supervisor
(Prof. Sunil Mohan)
IIT (BHU), Varanasi
INDIA

DECLARATION BY THE CANDIDATE

I "**Pooja Verma**", certify that the work embodied in this thesis is my own bona fide work and carried out by me under the supervision of "**Prof. Rajnesh Tyagi**" from "**July 2017** to **July 2023**", at the "**DEPARTMENT OF MECHANICAL ENGINEERING**", Indian Institute of Technology (BHU), Varanasi. The matter embodied in this thesis has not been submitted for the award of any other degree/diploma.

I declare that I have faithfully acknowledged and given credits to the research workers wherever their works have been cited in my work in this thesis. I further declare that I have not willfully copied any other's work, paragraphs, text, data, results, *etc.*, reported in journals, books, magazines, reports dissertations, theses, *etc.*, or available at websites and have not included them in this thesis and have not cited as my own work.

Date: 04/10/2023

Place: Varanasi

(**Pooja Verma**)

CERTIFICATE FROM THE SUPERVISOR

This is to certify that the above statement made by the candidate is correct to the best of my knowledge

Supervisor
(Prof. Rajnesh Tyagi)
IIT (BHU), Varanasi
INDIA

Co-Supervisor
(Prof. Sunil Mohan)
IIT (BHU), Varanasi
INDIA

Head of Department

Department of Mechanical Engineering,

Indian Institute of Technology (BHU), Varanasi

विभागाध्यक्ष/HEAD

यांत्रिक अभियान्तिकी विभाग/Deptt. of Mechanical Engg.

भारतीय प्रौद्योगिकी संस्थान/Indian Institute of Technology

(का०हि०वि०/B.H.U.)

सं.सं.सं. २२९००५/Varanasi-221005

COPYRIGHT TRANSFER CERTIFICATE

Title of the Thesis: *Studies on erosive wear characteristics of dual phase steel*

Name of the Student: POOJA VERMA

Copyright Transfer

The undersigned hereby assigns to the Indian Institute of Technology (Banaras Hindu University), Varanasi all rights under copyright that may exist in and for the above thesis submitted for the award of the "**DOCTOR OF PHILOSOPHY**".

Date: 04/10/2023

Place: Varanasi



(**POOJA VERMA**)

Note: However, the author may reproduce or authorize others to reproduce material extracted verbatim from the thesis or derivative of the thesis for author's personal use provided that the source and the Institute's copyright notice are indicated.

ACKNOWLEDGEMENT

The author is pleased to express her sincere regards and gratitude beyond words to her supervisor Prof. Rajnesh Tyagi and co-supervisor Prof. Sunil Mohan for their consistent help, encouragement, and valuable discussions during the entire period of her research work. The author would not have been able to complete the thesis without their utmost involvement and invaluable efforts. They motivated the author to pursue research problems and the need for persistent effort to accomplish the goal. The author is truly indebted to them.

Besides supervisors, the author would like to thank her RPEC members, Prof. R. K. Gautam and Prof. K. K. Singh for their insightful comments and encouragement. The author acknowledges her deep sense of gratitude to the current and former Heads of the Department of Mechanical and Metallurgical Engineering for providing all the research facilities to accomplish her research in the Department successfully. The author has an immense sense of gratitude to all the faculty members of the Department of Mechanical and Metallurgical Engineering, IIT (BHU), Varanasi for their cooperation and inspiration.

The author is thankful to the unknown reviewers who have rejected my papers several times in international conferences and journals. The comments that they provided helped to polish our articles in better shape. Nevertheless, the bigger and nobler cause of thanking them is that the rejections have equipped me with a high level of patience and helped me to implement my spiritual thoughts in practice. My acknowledgment will never be complete without the special mention to my lab seniors

and colleagues for their great help during five years of the Ph.D. journey- Dr. Rohit Kumar Singh Gautam, Dr. Manish Kumar, Dr. Hemant Nautiyal, Dr. Sudesh Singh, Dr. Ashwani Ranjan, Dr. Visweswara Rao Chukkala, Dr. Vikas Shivam, Dr. Rabindra Prasad, Dr. Akash Awale, Dr. Sanjay Gupta, Mr. Basudeb Rajak, Mr. Asgar Shakil, Mr. Roopchand Tandon, Dr. Dheeraj Jaiswal, Dr. Mudila Dhanunjaya Rao, Mr. Mithlesh Kumar Mahto, Mr. Nitish Mahto, Mr. Smita Gupta, Mr. Abhay Kumar, and especial thanks to my sister Dr. Preeti Verma and friends Mr. Adarsh Kumar, Ms. Seema Kumari, Ms. Swetha Rayala, and Ms. Munmun Agrawal with whom I started my journey at IIT (BHU), Varanasi. I convey my gratitude to all my teachers throughout my academic career for preparing me to walk through this long journey. The author is also thankful to all the lab, workshop, CIFC, and office staff of the department, especially Mr. Vijay Pratap Srivastava (CAM lab) and Kamlesh Mishra (MMD lab). I want to thank the administrative personnel at IIT BHU for helping me with their expertise during several requirements that had to be met over the entire course of the Ph.D. at IIT BHU.

Last but not least, words fail me to express my appreciation when it is time to share my gratitude to those very special people who always stood like a pillar of strength, my grand-mother Smt. Radha Verma, my parents Shri Surendra Verma and Smt. Meera Verma, sister Anjali Verma, and my continuous supporter Dr. Devashish Rajpoot for their unconditional support and encouragement to pursue my interest.

At last, regards to the almighty God who has given the author spiritual support and courage to carry out this work.

Sincerely

(POOJA VERMA)

CONTENTS

Contents	vi-x
List of Figures	xi-xv
List of Tables	xvi
List of Abbreviations/Symbols	xvii-xix
Preface	xx-xxvii
CHAPTER 1: INTRODUCTION	1-6
CHAPTER 2: REVIEW OF LITERATURE	7-51
2.1 Dual Phase Steel and their Properties	7
2.1.1 Different Phases of Steel	8-9
2.1.2 Types of Dual Phase Steels	10
2.1.2.1 Plain Carbon Dual Phase Steel	10
2.1.2.2 Alloyed Dual Phase Steel	10
2.1.3 Development of Dual Phase Microstructure	11
2.1.3.1 Intercritical Annealing	11
2.1.3.2 Direct Hot Rolling Technique	12
2.1.4 Mechanical Properties of Dual Phase Steel	13-15
2.1.4.1 Continuous Yielding of Dual Phase Steel	13
2.1.4.2 Yield Strength and Tensile Strength	14
2.1.4.3 High Rates of Work Hardening	16
2.1.4.4 High Uniform and Total Elongation	17
2.2 Wear and its Types	18
2.3 Erosive Wear of Metals	20

2.3.1 Solid Particle Erosion	20
2.3.2 Models for Erosion of Materials	21-24
2.3.2.1 Cutting Models	21
2.3.2.2 Localization Models	22
2.3.2.3 Fatigue Models	23
2.3.2.4 Adiabatic Shear Induced Spalling Models	24
2.3.3 Factors Affecting Solid Particle Erosion	24-28
2.3.3.1 Erodent Shape and Size	25
2.3.3.2 Properties of Erodent Material	26
2.3.3.3 Erodent Flow Rate	27
2.3.3.4 Impact Velocity	28
2.3.3.5 Impact Angle	29
2.3.3.6 Properties of Target Material	30
2.3.3.7 Temperature	31
2.3.4 Mechanism of Erosion	32-36
2.3.4.1 Erosive Wear by Plastic Deformation	33
2.3.4.2 Erosive Wear by Brittle Fracture	36
2.4 Erosive Wear of Steels	37-39
2.5 Corrosion	40-40
2.5.1 Types of Corrosion	40
2.5.1.1 Galvanic Corrosion	40
2.5.1.2 Uniform Corrosion	41
2.5.1.3 Crevice Corrosion	41
2.5.1.4 Pitting Corrosion	42
2.5.1.5 Intergranular Corrosion	42
2.5.1.6 Erosion Corrosion	42
2.5.1.7 Stress Corrosion Cracking	43
2.5.2 Factors Affecting Corrosion of Materials	43-45
2.5.2.1 Reactivity of Metal	43

2.5.2.2 Strain in Metal	44
2.5.2.3 Presence of Impurities	44
2.5.2.4 Presence of Electrolyte	44
2.5.2.5 Conditioning Gases and Moisture	45
2.5.2.6 Environmental Conditions	45
2.5.3 Corrosion of Dual Phase Steel	45-48
2.6 Formulation of the Problem	48-50
2.7 Objectives of the Study	51
CHAPTER 3: MATERIALS AND EXPERIMENTAL METHODS	52-70
3.1 Selection of Steel	52
3.2 Determination of Chemical Composition of Steel	52
3.3 Experimental Set-Up for Heat Treatment	53
3.4 Heat Treatment Variables and Procedure	54-58
3.4.1 Normalizing	55
3.4.2 Intercritical Annealing	56
3.5 Metallographic Studies	58-60
3.5.1 Optical Microstructural Examination	58
3.5.2 Scanning Electron Microscopy	59
3.5.3 Transmission Electron Microscopy	59
3.5.4 Atomic Force Microscopy	60
3.5.5 X-Ray Diffraction	60
3.6 Measurement of Mechanical Properties	61-62
3.6.1 Hardness Measurement	61
3.6.2 Tensile Testing	62
3.7 Fractographic Studies	62
3.8 Erosive Wear Testing	63-67
3.8.1 Impact Velocity Calibration	64
3.8.2 Erosion Test Procedure	66

3.9 Corrosion Studies	67
3.10 Examination of Eroded and Corroded Surface and Sub-Surface	70
CHAPTER 4: MECHANICAL PROPERTIES, EROSION AND CORROSION BEHAVIOR OF DP STEELS	71-117
4.1 RESULTS: Microstructure and Mechanical Properties	71-82
4.1.1 Chemical analysis and heat treatment of medium carbon steel	71
4.1.2 Microstructural Analysis	73
4.1.2.1 Optical Microscopy	73
4.1.2.2 Scanning Electron Microscopy	75
4.1.2.3 Transmission Electron Microscopy	76
4.1.2.4 X-Ray Diffraction Analysis	78
4.1.3 Mechanical Properties	78
4.2 RESULTS: Erosive Behavior of Steels	82-99
4.2.1 Examination of Eroded Surfaces	85
4.2.2 Discussion	90
4.3 RESULTS: Corrosion Behavior of Steel	99-117
4.3.1 Potentiodynamic Polarization and Gravimetric Analysis	99
4.3.2 Electrochemical Impedance Spectroscopy (EIS) Analysis	102
4.3.3 Scanning Electron and Atomic Force Microscopy	104
4.3.4 Discussion	110
CHAPTER 5: EROSION BEHAVIOR OF DP STEELS AT DIFFERENT IMPACT ANGLES AND VELOCITIES	118-145
5.1 Results	118
5.1.1 Erosive Wear at Different Impact Velocity and Angles	118-125
5.1.2 Examination of Eroded Surface	125-134
5.2 Discussion	134-145
CHAPTER 6: CONCLUSIONS	146-153

6.1 Mechanical Properties	146
6.2 Erosion Behavior at a Fixed Velocity and Different Impact Angles	147
6.3 Corrosion Behavior	149
6.4 Erosion of DP Steels at Different Impact Angles and Velocities	150
Future Scope	154
References	155-163
List of Publications	164

LIST OF FIGURES

Figure 2.1	Schematic representing the intercritical annealing heat treatment routes to develop high strength steel	11
Figure 2.2	Estimated equilibrium phase diagram and volume fraction austenite at intercritical temperatures	12
Figure 2.3	Figure 2.8 (a) Failed helicopter in the war and (b) Ingestion of dust at a runway in a desert	20
Figure 2.4	Typical dependence of erosion rate on impact angle for ductile and brittle materials	34
Figure 2.5	The impact direction was from left to right. (a) Ploughing deformation by a sphere; (b) type I cutting by an angular particle, rotating forwards during impact; (c) type II cutting by an angular particle, rotating backwards during impact	35
Figure 3.1	Schematic of vertical tube furnace for intercritical annealing time heat treatment	54
Figure 3.2	(a) Schematic indicating TTT diagram indicating heat treatment methods used to obtain DP steels and (b) Schematic shows the two phase region in the Iron rich portion of iron - iron carbide phase diagram	55
Figure 3.3	Geometry of Erosion test specimen	56
Figure 3.4	Schematic representation of intercritical annealing cycle	57
Figure 3.5	Layout for development of dual phase steel	58
Figure 3.6	Schematic diagram of dumbbell shaped tensile specimen	62
Figure 3.7	(a) Set-up of air jet erosion test rig and (b) Specimen holder for impact at different angles	63
Figure 3.8	Representation of Double disc arrangement set up	65

Figure 3.9	Representation of uncertainty in the impact velocity against the pressure.	67
Figure 3.10	Schematic of polarization cell for electrochemical behavior measurement	68
Figure 4.1	(a) Schematic of layout indicating heat treatment routes followed to develop normalized, dual phase and fully martensitic steels and (b) Variation of martensite volume fraction (%) with intercritical annealing time (sec)	73
Figure 4.2	Optical micrographs of (a) N steel, (b) DP2 steel, (c) DP3 steel, (d) DP3.5 steel, (e) DP4 steel and (f) FMS at a magnification of 100 X	75
Figure 4.3	Backscattered SE micrographs of (a) N steel showing ferrite and pearlite and (b) magnified view of (a) indicating pearlite colonies and (c) DP4 steel showing martensite islands in bright matrix of ferrite	76
Figure 4.4	Transmission electron micrographs of (a) N steel at 6.7 kX and inset at 13.7 kX magnification and (b) DP3.5 steel at 6.7 kX and inset at 26.7 kX and 13.7 kX magnification	77
Figure 4.5	XRD patterns of the N steel, DP steels, and FMS, respectively	78
Figure 4.6	Variation of Vickers hardness with ICA time (a) for the DP steels and (b) for the phases, martensite and ferrite	79
Figure 4.7	Engineering stress-strain plot for the N and DP steels	80
Figure 4.8	Fractographs of N, DP and FMS steels	82
Figure 4.9	Variation of steady state erosion rate with (a) impact angle and (b) hardness for the N and DP steels at a constant impact velocity of 90 m/s	83
Figure 4.10	Scanning electron micrographs of the worn surface of N and DP steels eroded at 15°	86
Figure 4.11	Scanning electron micrographs of the worn surface of N and DP steels eroded at 45°	87
Figure 4.12	Scanning electron micrographs of the worn surface of N and DP steels	88

	eroded at 75°	
Figure 4.13	Scanning electron micrographs of the worn surface of N and DP steels eroded at 90°	90
Figure 4.14	Schematic diagram of carbon concentration profile during initial stage of intercritical austenitization of carbon steel (C0) at 745 °C and (b) Fe rich portion of Fe-C phase diagram	91
Figure 4.15	Erosion scar of eroded surface of the DP4 steel at (a) 15°, (b) 45°, (c) 75° and (d) 90° angle of impingement	95
Figure 4.16	Schematic diagram for erosion mechanism at 45° IA.	97
Figure 4.17	Schematic diagram for erosion mechanism at 90° IA.	99
Figure 4.18	(a) Potentiodynamic polarization curve and (b) Gravimetric method data of N and DP steels in 3.5% NaCl solution for the corrosion	101
Figure 4.19	(a) Nyquist plot with the inset of Electrical Equivalent Circuit (EEC) model and (b) Bode plot for N and DP steels	104
Figure 4.20	SEM micrographs, EDS spectra and EDS maps of corroded surfaces of N and DP steels in 3.5% NaCl solution	107
Figure 4.21	Elemental distribution of (a, b & c) N and (d, e & f) DP3.5 steels after corrosion	108
Figure 4.22	Three-dimensional AFM images of the N steel and DP steels after corrosion	110
Figure 4.23	Schematic diagrams illustrating the corrosion mechanism of N, DP3.5 and DP4 steels exposed to 3.5 % NaCl solution.	116
Figure 5.1	Variation of erosion rate with time for (a) 15° and 30 m/s, (b) 15° and 120 m/s, (c) 90° and 30 m/s, and (d) 90° and 120 m/s	120
Figure 5.2	Variation of steady state erosion rate with initial hardness for impact velocity of 30 m/s, 60 m/s, 90 m/s 120 m/s, and at an impact angles of (a)	122

15°, (b) 45°, (c) 75°, and (d) 90°, respectively

- Figure 5.3** Variation of steady state erosion rate with impact velocity for the N steel, DP steels and FMS at impact angles of (a) 15°, (b) 45°, (c) 75°, and (d) 90°, respectively **123**
- Figure 5.4** Variation of steady state erosion rate with impingement angle for the N steel, DP steels and FMS at impact velocities of (a) 30 m/s, (b) 60 m/s, (c) 90 m/s, and (d) 120 m/s, respectively **125**
- Figure 5.5** SEM micrographs of eroded surface of (a) N steel, (b) DP2 steel, (c) DP3 steel, (d) DP3.5 steel, (e) DP4 steel, and (f) FMS at 30 m/s and 15° angle of impact **126**
- Figure 5.6** SEM micrographs of eroded surface of (a) N steel, (b) DP2 steel, (c) DP3 steel, (d) DP3.5 steel, (e) DP4 steel, and (f) FMS at 30 m/s and 90° angle of impact **128**
- Figure 5.7** SEM micrographs of eroded surface of (a) N steel, (b) DP2 steel, (c) DP3 steel, (d) DP3.5 steel, (e) DP4 steel, and (f) FMS at 120 m/s and 15° angle of impact **129**
- Figure 5.8** SEM micrographs of eroded surface of (a) N steel, (b) DP2 steel, (c) DP3 steel, (d) DP3.5 steel, (e) DP4 steel, and (f) FMS at 120 m/s and 90° angle of impact **130**
- Figure 5.9** SEM micrographs of cross section of (a) N steel, (b) DP3.5 steel, and (c) FMS, respectively, at 120 m/s and 15° angle of impact **132**
- Figure 5.10** SEM micrographs of cross section of (a) N steel, (b) DP3.5 steel, and (c) FMS respectively, at 30 m/s and 90° angle of impact **133**
- Figure 5.11** SEM micrographs of cross section of (a) N steel, (b) DP3.5 steel, and (c) FMS respectively, at 120 m/s and 90° impact angle **134**
- Figure 5.12** Micro-hardness profile of the eroded specimens of the N steel, DP3.5 steel **134**

and FMS at 15 and 90° angle of impact at (a) 30 m/s and (b) 120 m/s impact velocity

Figure 5.13 Schematic showing the proposed mechanism of material removal for (a) **142**
N steel, (b) DP3.5 steel, and (c) FMS at 15° and 120 m/s impact velocity

Figure 5.14 Schematic showing the proposed mechanism of material removal for (a) **144**
N steel, (b) DP3.5 steel, and (c) FMS at 90° and 120 m/s impact velocity

LIST OF TABLES

Table 3.1	Operating parameters for erosion test	67
Table 4.1	Chemical composition of as received steel	72
Table 4.2	Mechanical properties of Steels	81
Table 4.3	Summary of results obtained from potentiodynamic polarization tests	100
Table 4.4	Parameters of the equivalent electrical circuit (EEC) model	103
Table 4.5	AFM-Height parameters for corroded specimens	109
Table 5.1	Different conditions used for analysis of eroded surfaces	125
Table 5.2	Estimated values of Plot at different impact velocities for normal impact angle	137
Table 5.3	Estimated values of $\dot{\epsilon}$ (strain rate) at different impact velocities for N, DP2, DP3, DP3.5, DP4 and FMS steels	139

LIST OF ABBREVIATIONS/SYMBOLS

DP	Dual phase
N	Normalized steel
FMS	Fully martensitic steel
UTZ	Uniform temperature zone
MVF	Martensite volume fraction
SSER	Steady state erosion rate
PDP	Potentiodynamic polarization
EIS	Electrochemical impedance spectroscopy
OCP	Open circuit potential
CR	Corrosion rate
ICA	Intercritical Annealing
CPE₁	constant phase element
UTS	Ultimate tensile strength
AFM	Atomic force microscopy
EDX	Energy dispersive X-ray spectroscopy
HV	Vickers hardness
SEM	Scanning electron microscopy
TEM	Transmission electron microscopy
XPS	X Ray photoelectron spectroscopy
XRD	X-Ray diffraction spectroscopy
CNTD	Controlled nucleation thermochemical deposition
SCC	Stress corrosion cracking
% EL	Percent elongation
KE	Kinetic energy
E_{corr}	Corrosion potential

I_{corr}	Corrosion current
k	Erosion rate constant
V	Impact velocity
n	Velocity exponent
W	Wear rate
W_D	Volume loss
M	Total mass
V_p	Velocity of impinging particles
δ	Energy needed to remove a unit volume of material
ϵ_m	Mean strain increment
ρ_p	Particle density
C_p	Target specific heat
T_m	Melting point of target material
H_t	Static hardness of the metal or alloy
ϵ_{vp}	Erosion rate
$\Delta\Omega_m$	Mean strain increment induced by each impact
Ω_c	Critical strain for the onset of lip formation
R_s	Solution resistance
R_{pr}	Polarization resistance
P_{tot}	Total probability of first-order collision between the incident and a rebound particle
Q_o	Incident particle number flux
t_r	Average flight time of the rebounding particle
$\dot{\epsilon}$	Mean strain rate
γ	Austenite phase
m	Martensite phase

σ_y	Yield strength
σ_T	Tensile strength
V	Volume fraction
σ_u	Ultimate tensile strength
D	Average particle size
ε	True strain
K	Constant of order unity
r	Radius of martensite islands
l	half-length of martensite islands
G	Shear modulus
σ	True stress
b	Burgers vector
V	Impact velocity
k	Constant,
n	Velocity exponent
μ	Friction coefficient